

Determination of the asymptotic D - to S -state ratio of the triton from sub-Coulomb (\vec{d}, t) reactions

B. Kozłowska,* Z. Ayer, R. K. Das,† H. J. Karwowski, and E. J. Ludwig

Department of Physics and Astronomy, University of North Carolina at Chapel Hill, Chapel Hill, North Carolina 27599 and Triangle Universities Nuclear Laboratory, Durham, North Carolina 27708

(Received 5 July 1994)

Angular distributions of the tensor analyzing power A_{zz} have been measured for ground state transitions in $^{119}\text{Sn}(\vec{d}, t)^{118}\text{Sn}$ and $^{149}\text{Sm}(\vec{d}, t)^{148}\text{Sm}$ and the first excited state (0.263 MeV) in $^{206}\text{Pb}(\vec{d}, t)^{205}\text{Pb}$ for deuteron energies well below the Coulomb barrier. Exact, finite-range distorted-wave Born approximation analyses of these data have been made to establish the asymptotic D - to S -state ratio for the triton, η_t . These calculations include a deuteron-nucleus tensor potential determined from the folding model and a long-range tensor potential arising from the Coulomb interaction. Previously obtained $A_{zz}(\theta)$ data for the ground state transitions in $^{95}\text{Mo}(\vec{d}, t)^{94}\text{Mo}$, $^{119}\text{Sn}(\vec{d}, t)^{118}\text{Sn}$, and $^{149}\text{Sm}(\vec{d}, t)^{148}\text{Sm}$ at different sub-Coulomb energies have been reanalyzed. Also a careful investigation of possible uncertainties in the value of η_t is presented. A best fit to the data gives $\eta_t = -0.0411 \pm 0.0013 \pm 0.0012$, somewhat lower than previous experimental determinations.

PACS number(s): 21.45.+v, 24.50.+g, 24.70.+s, 25.45.Hi

I. INTRODUCTION

The three-nucleon problem has been the subject of extensive experimental and theoretical studies for more than two decades. Within the last few years considerable progress has been made in understanding properties of the bound-state system. Exact Faddeev-type equations for realistic Hamiltonians based on two- and three-body forces aimed at determining the properties of three-nucleon systems were solved. This enables one now to attempt meaningful comparisons between theory and experiment and makes possible an investigation of the fundamental physics that underlies the structure of the three-nucleon system. In spite of recent progress in experimental and theoretical work a complete understanding of the three-nucleon system has not yet been achieved.

Measurements of tensor analyzing powers (TAP's) as described in the present paper provide unique information about few-nucleon systems, especially the tensor force component of the nucleon-nucleon (NN) interaction. TAP's calculated for (\vec{d}, t) reactions at sub-Coulomb energies strongly depend upon the D -state am-

plitude of the $n+d$ component in the triton wave function and have magnitudes roughly proportional to η_t , the ratio of D - to S -state asymptotic wave functions for the triton [1]. Since the percentage D state is not a physical observable, an accurate η_t determination is an important measure of the D -state amplitude and a test of calculations of few-nucleon systems using "realistic" two-body and three-body forces [2-4].

A determination of η_t using transfer reactions at sub-Coulomb energies has been made by this group previously [5]. Angular distributions of the TAP's A_{zz} and A_{yy} for three different targets and four incident energies were analyzed using a finite-range distorted-wave Born approximation (DWBA) analysis. In the present work we extract η_t using an enlarged data set and an improved analysis method. This new determination is based on previously reported angular distributions of A_{zz} as well as three new A_{zz} measurements, including two obtained at much lower energies than before (41% and 43% below the Coulomb barrier). The analysis of the new low-energy data is more precise and more reliable due to the reduced sensitivity of DWBA calculations to optical model parameters. The ambiguities inherent in optical-model-based analyses as well as experimental errors and beam polarization instability were carefully investigated for all data sets analyzed in the present work. Some minor improvements of experimental techniques over those used in Ref. [5] provided cleaner spectra, reducing the uncertainty in the experimental A_{zz} values.

The next section contains the summary of previous experimental and theoretical determinations of η_t . Section

*Present address: Physics Department, University of Silesia, Katowice, Poland.

†Present address: Radiation Oncology Center, Mallinckrodt Institute of Radiology, Washington University School of Medicine, St. Louis, MO 63110.

III contains the description of the experimental procedure. The DWBA analyses together with the final result are presented in Sec. IV. Results are discussed in Sec. V.

II. OVERVIEW

One of the most interesting manifestations of the two-nucleon tensor force is the presence of an $l = 2$ component in the ground states of light nuclei. The existence of the quadrupole moment for the deuteron (Q_d) is associated with the presence of a D state and has been known for decades. Analyses of low-energy n - p scattering experiments reveal that the tensor force accounts for 70% of the binding interaction in the deuteron [6].

Measurements of cross section and vector and tensor analyzing powers in (\vec{d}, p) reactions were successfully applied by the Wisconsin group [7–10] to determine the asymptotic D - to S -state normalization ratio for the deuteron, η_d . Calculated values of Q_d and η_d agree with experiment within a few percent when only the one-pion-exchange part of the nucleon-nucleon tensor interaction is considered. The same force is responsible for approximately 50% of the binding energy of ${}^3\text{H}$ and ${}^3\text{He}$ [6] and generates significant D -state components in these nuclei. However, unlike the deuteron, ${}^3\text{H}$ and ${}^3\text{He}$ have spin $\frac{1}{2}$ and do not possess a quadrupole moment, so normalization constants remain as the only D -state-dependent observables to be investigated.

The first experimental studies of a D -state component in the triton wave function were carried out using (\vec{d}, t) reactions with deuteron energies both above and below the Coulomb barrier [11–13]. The DWBA calculations were made using the local energy approximation (LEA) which approximates the finite-range effects at the ${}^3\text{H} \rightarrow d + n$ vertex. The first attempt to evaluate the range of validity of the LEA was made by Ioannides, Nagarajan, and Shyam [14]. They showed that predicted values of the tensor analyzing power T_{20} for backward angles are reduced by almost 30% when one uses the LEA instead of a full finite-range calculation and therefore the use of this approximation is not adequate for precise TAP calculations.

The effect of the deuteron-nucleus tensor force was first included in calculations of analyzing powers in (\vec{d}, t) reactions by Karban and Tostevin [15]. They found that in general the addition of an optical model (OM) tensor potential does not change the shape but increases the magnitude of calculated TAP angular distributions and concluded that this term cannot be neglected for either sub-Coulomb or near-barrier incident deuteron energies. Some recent studies involve full finite-range DWBA calculations together with an OM tensor potential, although the experiments were carried out with beam energies well above the Coulomb barrier [16,17].

A more recent attempt at establishing a precise value of η_t was made by Das *et al.* [5]. Angular distributions of A_{zz} and A_{yy} were measured in the ${}^{95}\text{Mo}$, ${}^{119}\text{Sn}$, and ${}^{149}\text{Sm}$ (\vec{d}, t) reactions for deuteron energies below the Coulomb barrier. An exact finite-range DWBA analy-

sis was performed which included a complex tensor potential. The possible effects of the Coulomb field of the target on the deuteron and triton wave functions were estimated to give a contribution of 4% to the total error, resulting in $\eta_t = -0.043 \pm 0.002$. Results of another recent determination of η_t using an experimental method and theoretical calculations similar to those of Das *et al.* were published by George and Knutson [18]. They measured T_{20} and T_{21} for four different target nuclei at energies from 46% to 21% below the Coulomb barrier. They performed an extensive evaluation of the uncertainty in η_t and obtained a value for $\eta_t = -0.0431 \pm 0.0025$. A determination from the extrapolation method of TAP's to the nucleon-transfer pole was made by Vuaridel *et al.* [19] yielding a value of $\eta_t = -0.050 \pm 0.006$. However, Londergan, Price, and Stevenson [20] have questioned this technique as one which underestimates the actual errors.

Theoretical predictions of η_t have improved dramatically in precision over the last decade [2–4]. Modern calculations of fundamental three-nucleon properties such as binding energy η , electromagnetic form factors, and charge radii have been performed using realistic NN potentials, with and without the $3N$ interaction, by numerically solving the Faddeev equations. The results of those calculations are often presented as plots of predicted low-energy observables as a function of predicted binding energy (E_B) for different NN potentials (so-called Phillips line). A linear dependence of η_t , as well as other observables, on binding energy is found [2,4] from which a best value of η_t can be obtained by least-squares fitting at the experimentally determined $E_B({}^3\text{H}) = 8.48$ MeV. In such a way Ishikawa and Sasakawa [2] found $\eta_t = -0.0432 \pm 0.0015$ and Friar *et al.* [4] obtained $\eta_t = -0.046 \pm 0.001$. Therefore a precise experimental η_t determination is of considerable importance since it can discriminate between different theoretical wave functions obtained by solving the Faddeev equations and hopefully provide information about effects of $3N$ forces.

III. EXPERIMENTAL PROCEDURE

The tensor analyzing power $A_{zz}(\theta)$ was measured in (\vec{d}, t) reactions on ${}^{119}\text{Sn}$, ${}^{149}\text{Sm}$, and ${}^{206}\text{Pb}$ targets. Experiments were performed at the Triangle Universities Nuclear Laboratory (TUNL) using the high-intensity Atomic Beam Polarized Ion Source (ABPIS) [21]. In order to obtain a theoretical tensor polarization $p_{zz} = -1$ (state 3), a strong field transition unit was used while $p_{zz} = +1$ (state 2) was obtained using a medium field unit. The atoms were ionized in an electron-cyclotron resonance ionizer and negatively charged in a cesium oven. The desired spin precession was obtained in a Wien filter. The ABPIS provided the negatively charged polarized deuterons with typical polarizations $p_{zz} = \pm 0.70$. After acceleration in the 10 MV FN Tandem, the beam was sent to a 62 cm scattering chamber. After passing through the target the beam polarization was analyzed in a polarimeter utilizing the ${}^3\text{He}(\vec{d}, p){}^4\text{He}$ reaction [22]. Beam currents on target were typically in the range 0.5–1.0 μA .

Targets used in the experiments were self-supporting foils made from isotopically enriched materials. The isotopic purity for all targets was in a range of 99.4–99.8%. Particles scattered from the target were detected and identified using ΔE - E telescopes consisting of silicon surface-barrier detectors. The telescopes consisted of ΔE transmission detectors with thicknesses in a range 50–300 μm depending on the energy range of the tritons, followed by an E detector, thick enough to stop the tritons. Three pairs of telescopes were symmetrically placed with respect to the incident beam direction. The telescopes subtended a solid angle of 3 msr and were separated by 10° or 15° in different experiments in which angular distributions were taken in steps of 5° or 7.5° .

An improvement over the experimental techniques described in Ref. [5] was made by using a shorter coincidence resolving time (50 ns as opposed to 500 ns) to produce cleaner charged-particle spectra. Also fast (< 0.5 s) spin-state switches between states 2, 3 and the unpolarized state were carried out under computer control in contrast to the manual changes made previously at intervals of about 45 min. With this new method, data for each spin state were acquired almost simultaneously so slow changes in experimental parameters such as beam position on target, amplifier gain, and target thickness affect the spectra for each state in the same way.

To obtain experimental values of the tensor analyzing power A_{zz} , peak sums for left and right detectors were added together. This procedure has the advantage that it compensates to first order for the effects of left-right shift of the beam position on target. A_{zz} was calculated from the expression

$$A_{zz} = \frac{2(R - 1)}{(p_{zz}^{(2)} - Rp_{zz}^{(3)})^2},$$

where

$$R = \frac{L^{(2)} + R^{(2)}}{L^{(3)} + R^{(3)}},$$

for the left (L) and right (R) detectors placed at the same angle in the scattering chamber. The superscript denotes the polarization state. The 5–10% uncertainties in the TAP's result primarily from counting statistics.

Although for most of the experiments the tritons in the mass spectra were well separated from deuterons, they were not free from background produced by processes such as pulse pileup. In addition to statistical uncertainties, the uncertainties in analyzing powers include small contributions from statistical uncertainties in the beam polarization. There was also an overall scale error of 3% from polarimeter calibration uncertainties [22]. The contribution of this uncertainty to the determination of η_t is considered separately. The results of the tensor-analyzing-power measurements for ^{119}Sn , ^{149}Sm , and ^{206}Pb targets are presented in Fig. 1. The solid lines are the results of finite-range distorted-wave Born approximation calculations which are described in the next section.

IV. ANALYSIS

A. DWBA calculations

The analysis of (\vec{d}, t) reactions on medium-weight and heavy nuclei using exact, finite-range DWBA calculations has been described previously [5,17]. Since DWBA theory is utilized to determine η_t , it is important to maintain certain conditions to maximize the reliability of the theory. Reactions at sub-Coulomb energies with Q values close to zero tend to provide these conditions since particles at sub-Coulomb energies stay well outside of the nuclear surface. Choosing reactions for which the Q value is close to zero assures that the elastic-scattering wave functions are well matched in the region of the turning point of the classical Coulomb trajectories. Also at these energies the observed TAP results almost entirely from the triton D state and not from nuclear spin-dependent forces.

A systematic investigation of j dependence of TAP's in single nucleon transfer reactions was made by Bhat *et al.* [17]. They found that TAP's for $j = l + \frac{1}{2}$ transfers exhibit significantly more pronounced D -state effects

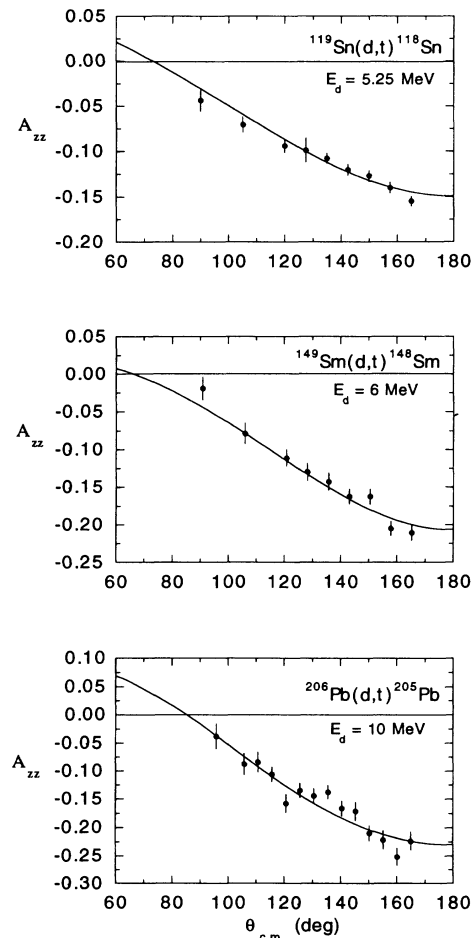


FIG. 1. Angular distributions of A_{zz} for the ^{119}Sn , ^{149}Sm , and ^{206}Pb (\vec{d}, t) reactions at sub-Coulomb incident energies. The solid curve is an exact, finite-range DWBA calculation using the best fit value of η_t given in Table III below.

than those for $j = l - \frac{1}{2}$ transfers and therefore only those were investigated in the present work. Moreover, in order to avoid the ambiguity of summing multiple- l -transfer spectroscopic amplitudes in the DWBA calculations, only reactions with unique l transfers were investigated. These reactions, three from the present work and four from Ref. [5], with their Q values and j^π transfers are listed in Table I.

The tensor analyzing power A_{zz} was calculated for reactions listed in Table I using the finite-range DWBA code PTOLEMY [23] which allows the inclusion of deuteron-nucleus optical-model tensor potentials in the entrance channel. The real and imaginary central potentials (V and W) and spin-orbit potential (V_{SO}) in the entrance channel were calculated from the global potential formulas of Daehnick, Childs, and Vrcelj [24], and exit channel potentials were taken from the work of Becchetti and Greenlees [25].

In addition to the central and spin-orbit parts of the deuteron potential, the nuclear tensor potential U_{TR} was also considered. The tensor potential has the form [26]

$$U_{TR} = [V_{TR}(r) + iW_{TR}(r)]T_r,$$

where

$$T_r = (\vec{s} \cdot \hat{r})^2 - \frac{2}{3}.$$

The proper determination of the parameters of U_{TR} is particularly important since calculations of tensor analyzing powers in the (\vec{d}, t) reactions are quite strongly affected by its choice. Unfortunately there are not enough data available to guide one in an unambiguous selection of U_{TR} . The folding model (FM) as proposed by Keaton and Armstrong [27] is commonly used to generate the tensor-potential parameters. There are, however, variations in the magnitudes of the parameters providing best fits to (d, d) polarization observables. In certain cases the full values from Keaton and Armstrong are used [28], while in others V_{TR} and W_{TR} are reduced by a factor of 2 [9], or one or the other is set to zero [29].

On the other hand, work by Tostevin [30] shows that the necessity to adjust arbitrarily the FM parameters to describe adequately TAP data in elastic scattering might result from a neglect of channel coupling. Tostevin showed that in the case of ^{208}Pb , the deuteron elastic-scattering data could be very well described if coupling

to the (\vec{d}, p) channels is taken into account, without any use of the FM tensor potential. Since there were no calculations done for the elastic scattering from other targets for which elastic-scattering data exist [9,28,29] or for those used in the present experiments, it is difficult to judge whether the coupled-channels effect is also present in these cases. However, some favorable conditions, such as low Q value for the (\vec{d}, p) reaction, high spectroscopic factors for transitions going to several excited states, or low angular momentum transfer, may enhance the effects of channel coupling.

Since the existing set of (\vec{d}, d) data at energies of interest here is very limited and the conclusions about the size and even presence of the tensor potentials inconsistent, it is not possible to adjust them to each individual reaction. Therefore, instead of arbitrarily scaling the parameters of the FM as has been done in Ref. [18], we have attempted to establish a simple procedure for generating the U_{TR} parameters in a consistent way. We follow here the prescription of Santos [31]. Neglecting the contribution of the Coulomb force to the nucleon-nucleus potentials, he proposed that the tensor interaction part of the OM potential be calculated as

$$U_{TR}(r) = Q_d DV(r)T_r,$$

where

$$D = r \left(\frac{1}{dr} \right) \left(\frac{1}{r} \frac{d}{dr} \right)$$

is the second-order differential operator in r , and $V(r)$ is the nucleon-nucleus optical potential. The $V(r)$ values at a neutron energy equal to half of the incident deuteron energy were taken from the extensive fits of Rapaport [32], obtained by optical-model analyses of neutron elastic-scattering data. Using this global parametrization for $V(r)$, the nuclear tensor-potential parameters were calculated for all reactions of interest and are listed in Table II.

TABLE II. The optical-model tensor-potential parameters used in the incoming channel. The radius and diffuseness parameters for all reactions are kept fixed at $r_{TR} = 1.198$ fm and $a_{TR} = 0.663$ fm for the real part and $r_{TRi} = 1.295$ fm and $a_{TRi} = 0.59$ fm for the imaginary part. The depths V_{TR} and W_{TR} are as defined in the folding model of Ref. [27]. For comparison, the folding model depths in Ref. [27] are $V_{TR} = 7.0$ MeV and $W_{TR} = 1.0$ MeV.

Reaction	E_d (MeV)	V_{TR} (MeV)	W_{TR} (MeV)
$d + ^{95}\text{Mo}$	7.00	7.219	0.600
	5.25	7.110	0.470
$d + ^{119}\text{Sn}$	6.00	7.100	0.490
	7.00	7.080	0.520
$d + ^{149}\text{Sm}$	6.00	7.077	0.477
	8.00	7.034	0.534
$d + ^{206}\text{Pb}$	10.0	6.880	0.525

TABLE I. Sub-Coulomb (\vec{d}, t) reactions investigated, with Q value and angular momentum transfer.

Target	E_d (MeV)	j^π	Q value (MeV)	% below V_C ^a
^{95}Mo	7 ^b	$\frac{5}{2}^+$	-1.11	13
^{119}Sn	5.25, 6 ^b and 7 ^b	$\frac{1}{2}^+$	-0.23	41, 33, and 22
^{149}Sm	6 and 8 ^b	$\frac{7}{2}^-$	0.38	43 and 24
^{206}Pb	10	$\frac{3}{2}^-$	-2.10	21

^a V_C represents the Coulomb barrier for deuterons calculated as $V_C = Z_t^* 1.44 / r_c^* (A_t^{1/3} + 2^{1/3})$ MeV.

^bMeasurements of Das *et al.* (Ref. [5]).

In addition to U_{TR} there exist two long-range tensor potentials which arise from the interaction between the electric field of the target nucleus and the deuteron. The first one arises from the interaction of the quadrupole moment of the charge distribution of the deuteron with the gradient of the electric field [29] and is expressed by

$$V_a = \frac{3}{2r^3} Q_d Z e^2 T_r .$$

The second tensor potential arises from the electric polarization of the deuteron in the Coulomb field of the target nucleus. This potential consists of the central and tensor terms and is given by [29]

$$V_p = -\frac{1}{2r^4} Z^2 e^2 (\alpha + 3\tau T_r) ,$$

where α and τ are the central and tensor polarizations, respectively. Only the tensor term is included in the present calculation since the central one has negligible effect on the analyzing powers and the value of τ was taken to be 0.0343 fm^3 following the prescription of Ref. [33]. Including these two potentials causes a change of a few percent in the calculated A_{zz} at sub-Coulomb energies.

B. Determination of η_t from the individual angular distributions

The quantity used to judge the quality of the agreement between calculated and measured observables is the function χ^2 defined by

$$\chi^2 = \sum_{i=1}^N \left(\frac{f_i(x) - y_i}{\Delta y_i} \right)^2 , \quad (1)$$

where x is the parameter being varied, f_i are calculated observables, y_i are data, Δy_i is the uncertainty in y_i , and N is the number of measurements. The results of the parameter variation and resulting uncertainties in η_t are described in the next section.

The values of η_t are extracted by minimizing the χ^2 parameter between calculated and measured TAP's for a given value of the parameter x . In this case, the parameter x is the value of the asymptotic D -state amplitude N_D (normalized with the S -state amplitude by the condition $N_S^2 + N_D^2 = 1$), the quantity $f(x)$ is the tensor analyzing power A_{zz} , and the χ^2 expression is given by

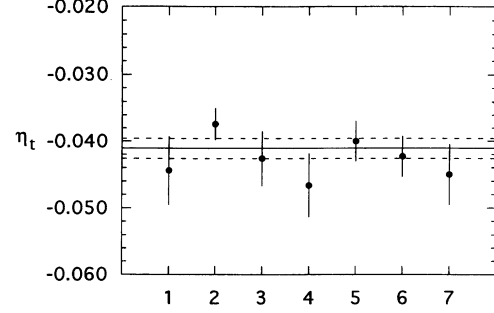


FIG. 2. Results of the η_t values obtained from the seven individual measurements, plotted in the same order as in Table III. The solid line represents the final η_t value obtained as the weighted average of the individual measurements, with the dashed lines the limits on the error of the final value.

$$\chi^2 = \sum_{i=1}^N \left(\frac{A_{zz}^{\text{th}}(N_D) - A_{zz}^{\text{exp}}}{\Delta A_{zz}^{\text{exp}}} \right)^2 , \quad (2)$$

where A_{zz}^{exp} are the measured TAP's with statistical uncertainties $\Delta A_{zz}^{\text{exp}}$ and A_{zz}^{th} are the corresponding DWBA calculations of A_{zz} using the global parameters of Daehnick, Childs, and Vrcelj [24], along with the tensor-potential parameters from Table II for the entrance channel, and OM potentials from Ref. [25] for the exit channel. The asymptotic D - to S -state ratio η_t was calculated for the D -state amplitude at which χ^2 was minimized. The results are summarized in Table III along with statistical uncertainties $\Delta \eta_t^S$ and the minimum χ^2 per degree of freedom (χ^2/N). It must be specified that each χ^2/N value results from the statistical uncertainty in the background subtraction and a 3% uncertainty in the overall normalization of the beam polarization. Figure 2 shows a comparison of the seven η_t determinations obtained from the seven individual measurements of A_{zz} (four from Ref. [5] and three from the present experiment). The values are plotted in the same sequence as they appear in Table III.

C. Uncertainty in the calculations

In addition to statistical errors listed in Table III, systematic errors in the determination of the η_t can arise from uncertainties in the theoretical calculations of A_{zz} . In order to assure the reliability of the DWBA calcula-

TABLE III. Results of the individual η_t measurements and the uncertainties associated with each measurement.

Target	E_d (MeV)	% below V_C	η_t	$\Delta \eta_t^S$	χ^2/N	$\Delta \eta_t^{\text{CSO}}$	$\Delta \eta_t^{\text{UTR}}$	$\Delta \eta_t^0$	$\Delta \eta_t$
^{95}Mo	7	13	-0.0444	0.0037	0.86	0.0020	0.0025	0.0013	0.0051
^{119}Sn	5.25	41	-0.0374	0.0020	1.42	0.0006	0.0004	0.0011	0.0024
^{119}Sn	6	33	-0.0426	0.0037	1.33	0.0006	0.0010	0.0013	0.0041
^{119}Sn	7	22	-0.0466	0.0031	1.41	0.0020	0.0026	0.0014	0.0047
^{149}Sm	6	43	-0.0400	0.0026	1.09	0.0006	0.0005	0.0012	0.0030
^{149}Sm	8	24	-0.0423	0.0020	0.90	0.0012	0.0013	0.0013	0.0030
^{206}Pb	10	21	-0.0450	0.0041	1.63	0.0010	0.0003	0.0014	0.0045

tions and to estimate resulting uncertainties it is necessary to test their sensitivity to the choice of optical-model potentials. To perform these tests the real and imaginary central, spin-orbit, and tensor-potential parameters were varied extensively and their effects on the elastic-scattering data were carefully studied. As mentioned above, the largest uncertainty is due to the choice of optical potentials used in the DWBA calculations and therefore in what follows the uncertainties in the calculations due to the real and imaginary central and real spin-orbit parts of the potential ($\Delta\eta_t^{\text{CSO}}$) and that due to the choice of tensor potential ($\Delta\eta_t^{\text{UTR}}$) are considered separately.

The uncertainty $\Delta\eta_t^{\text{CSO}}$ is given by

$$\Delta\eta_t^{\text{CSO}} = \left[\sum_{i=1}^N [\Delta\eta_t^i(x_i)]^2 \right]^{1/2}, \quad (3)$$

where x_i are the parameters varied in the calculations, i.e., real and imaginary central and real spin-orbit depths. To determine $\Delta\eta_t^{\text{CSO}}$ it is necessary to assign an uncertainty to each of the parameters used in the DWBA calculations.

The choice of central and spin-orbit potentials resulted from an analysis of differential cross-section $\sigma(\theta)$ and vector-analyzing-power (iT_{11}) data for the $^{208}\text{Pb}(\vec{d}, d)^{208}\text{Pb}$ scattering at $E_d=10$ MeV [34]. This case has been selected from a limited set of measurements of elastic scattering at sub-Coulomb energies available in the literature, because the target is very similar to ^{206}Pb and the $^{206}\text{Pb}(\vec{d}, t)^{205}\text{Pb}$ reaction is expected to be the most sensitive to variations in the OM parameters. Our measurements of this reaction were made at the highest deuteron bombarding energy (only 21% below the Coulomb barrier) studied as part of the present work and provide the upper limit of the relevant uncertainties.

Calculations of elastic-scattering observables were performed using the optical-model code DDTP [35]. Optical-model parameters from the global fit of Daehnick, Childs, and Vrcelj yielded a good description of the cross-section data ($\chi^2/N = 1.6$) but a poor description of vector-analyzing-power data. The calculated iT_{11} were about an order of magnitude smaller than the data.

The next step, in an effort to determine the validity of OM parameters, was to study the uncertainty in the deuteron V , W , and V_{SO} parameters (as defined in Ref. [24]) by varying their values from those of the global fit and finding the magnitude of the parameter which doubled the calculated χ^2 for $\sigma(\theta)$. This corresponded to a 20% variation in the depth of W and a 30% change in V . At the same time no changes were found for iT_{11} and only small changes were observed in T_{20} predictions (differences in the χ^2/N were less than 0.5). Applying as much as a 50% change to the V_{SO} depth parameter changes χ^2/N for iT_{11} by 1.0. Simultaneously, no change was noticed in the cross section and T_{20} fits. In view of the above results, in the subsequent (\vec{d}, t) reaction analysis allowance for variations of 20% were made for the imaginary term W , 30% for the real term V , and 50% for the spin-orbit term V_{SO} . Because of the lack of ex-

perimental triton elastic-scattering data at sub-Coulomb energies, the same uncertainty was adopted for both incident and outgoing channels.

The wave function of the neutron in the target nucleus was generated using the separation-energy method, where the neutron is assumed to be bound in a Woods-Saxon (WS) well. For a given value of well radius and diffuseness the potential depth was adjusted to give the correct binding energy of the neutron with the residual nucleus. The sensitivity of η_t to the choice of well geometry was tested by varying the well radius. The TAP predictions were insensitive to these parameters although the overall magnitude of the predicted cross section varied somewhat.

The radial form factors at the projectile vertex for the lighter system (which in this case is the deuteron with the neutron) were calculated using the same separation-energy method. It was assumed that for both the S and the D state the geometry is kept the same but potential depths are different. Different WS potential geometries produce bound-state neutron wave functions which differ inside the nuclear radius. At large radii they become appropriately normalized Hankel functions. The assumption that at sub-Coulomb energies the TAP's are sensitive only to the asymptotic region of the wave functions was found to be valid when WS geometrical parameters were varied by 20% and no effect in the calculated TAP's was observed. The net uncertainty in η_t was obtained by adding in quadrature the uncertainties due to individual parameter variations described above and is listed in Table III as $\Delta\eta_t^{\text{CSO}}$.

Since the OM tensor potential has an effect larger than the combination of all other OM parameters on the calculated analyzing powers, the uncertainty arising from its choice is considered separately. As mentioned in Sec. IV A the nucleon-nucleus potential $V(r)$ is obtained from global OM analyses [32] of neutron scattering from targets of interest in a range $0 < E_n < 5$ MeV. In order to determine the uncertainty arising from this specific choice of global neutron-nucleus potential, the calculations were also done for values of $V(r)$ taken from fits to neutron elastic-scattering data for individual target nuclei. Therefore, additional potentials for ^{95}Mo were taken from [36,37], for ^{119}Sn from [36,38], for ^{149}Sm from [36,38], and for ^{206}Pb from [39,40]. From the variations in the calculated η_t due to the different U_{TR} potentials generated we obtained deviations of the η_t values from those calculated using the parameters listed in Table II. These deviations, which are an estimate of the uncertainty resulting from the choice of tensor potential parameters, are listed in Table III as $\Delta\eta_t^{\text{UTR}}$.

The uncertainty in the Coulomb tensor potential and the stretching potential has a negligible effect on the uncertainty in the calculated η_t . The quadrupole moment of the deuteron as determined by atomic physics methods is more than adequately precise [$Q_d = 0.2859(3)$ fm²] and does not introduce an appreciable error in η_t . The 4% uncertainty in the tensor polarizability τ introduces less than 0.1% uncertainty in the calculated η_t and thus is also neglected.

An overall additional uncertainty of 3% in η_t was as-

sumed to take into account effects that were not investigated due to lack of reasonable input, such as virtual excitations in the triton wave function. A study of this effect on TAP's for sub-Coulomb (d, p) reactions was made by Tostevin and Johnson [41] who found that it contributes about 3% to the TAP magnitudes. One might expect smaller effects in (\bar{d}, t) reactions since the triton wave function alone strongly influences the TAP and tritons are less sensitive to Coulomb distortions than deuterons because of their larger binding energy. However, since these effects were never investigated for $3N$ systems, we assume the same uncertainty as for deuterons. The contribution to the uncertainty in η_t which arises from this effect is shown in Table III as $\Delta\eta_t^0$.

Summarizing, Table III lists the statistical uncertainties ($\Delta\eta_t^S$), uncertainties in the DWBA calculations ($\Delta\eta_t^{\text{CSO}}$) excluding the tensor potential, uncertainties arising from the choice of tensor potential ($\Delta\eta_t^{\text{UTR}}$), and the uncertainty due to other effects ($\Delta\eta_t^0$).

D. The final η_t result

The final value of the asymptotic D - to S -state ratio is obtained by combining together the seven individual results listed in Table III. As each result contains four different sources of uncertainty these were combined first to obtain a total uncertainty in each measurement by adding all individual errors in quadrature:

$$\Delta\eta_t = \left[(\Delta\eta_t^S)^2 + (\Delta\eta_t^{\text{CSO}})^2 + (\Delta\eta_t^{\text{UTR}})^2 + (\Delta\eta_t^0)^2 \right]^{1/2}. \quad (4)$$

It is interesting to note how the individual uncertainties contribute to $\Delta\eta_t$ for each measurement. The biggest uncertainty arises from statistics which varies from 5% of the value of η_t (for the present data) to about 10% (for data from Ref. [5]). The uncertainty due to the tensor potential, $\Delta\eta_t^{\text{UTR}}$, increases with the deuteron bombarding energy. It varies from 1.4% to almost 15% of the extracted value of η_t for the measurements taken at energies 43% below the barrier to 13% below the barrier, respectively. This uncertainty therefore strongly influences the weight given to different individual results in the final computation of η_t . Similar energy dependence is observed in $\Delta\eta_t^{\text{CSO}}$. However, this uncertainty does not contribute very strongly to the overall uncertainty $\Delta\eta_t$ because the DWBA calculations are not very sensitive to the choice of the central and spin-orbit potential parameters. In the worse case for ^{119}Sn at $E_d = 7$ MeV this uncertainty is about 3%. The last source of uncertainty, $\Delta\eta_t^0$, is assumed to be 3% for all individual measurements, as was discussed in the previous subsection.

The final value of η_t , $\bar{\eta}_t$, is obtained by computing a weighted average of the seven individual results, with the weighting factor being the inverse square of the error in each η_t measurement ($\Delta\eta_t$). The error in $\bar{\eta}_t$ is calculated

using standard error propagation formulas. There is an additional contribution to the error in $\bar{\eta}_t$ which arises from the uncertainty in the polarimeter calibration [22]. This is found to introduce an error of 3% in the value of $\bar{\eta}_t$. We thus obtain

$$\bar{\eta}_t = -0.0411 \pm 0.0013 \pm 0.0012,$$

where the first error is the combination of the errors in the individual measurements and the second error is due to the uncertainty in the beam polarization. This final result is shown by the solid line (with the dashed lines the error limits) in Fig. 2 together with the seven individual η_t determinations.

V. CONCLUSIONS AND SUMMARY

From comparison of the tensor analyzing powers measured from (d, t) reactions at sub-Coulomb energies with full finite-range DWBA calculations, η_t for the triton wave function is obtained. The value of η_t is equal to $-0.0411 \pm 0.0013 \pm 0.0012$. The uncertainty in the η_t determination includes statistical errors, theoretical calculation errors, estimates of errors due to effects not calculated, and the error in the beam polarization due to the polarimeter calibration uncertainty. The goal of the analysis has been to determine η_t with accuracy sufficient to be of use in distinguishing between various realistic NN interactions [3,4].

The experimental data sets used in the analysis included, in addition to data of Ref. [5], new measurements made mainly at lower incident energies (41% and 43% below the Coulomb barrier) to minimize the influence of the nucleon-nucleus interaction. Another improvement over the previous work comes from changes in the experimental technique used. The use of fast-coincidence electronics improved the quality of the charged-particle spectra, and the use of fast spin-state switching improved the accuracy of the measurements.

Considerable effort was made to estimate realistically the error arising from the uncertainty in tensor-potential parameters used in the DWBA calculations and a con-

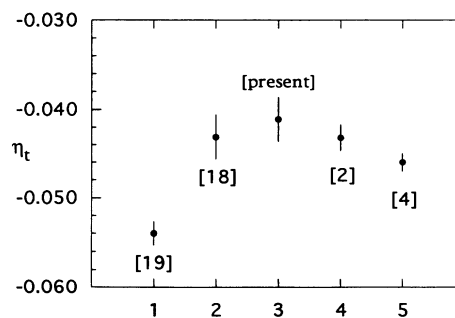


FIG. 3. Summary of recent experimental determinations and theoretical calculations of η_t . Reference [19] is the result obtained by Vuaridel *et al.*, [18] is the result obtained by George and Knutson, [2] is the Sendai group calculation, and [4] is the Los Alamos group calculation.

sistent approach was adopted to determine these parameters using the folding model. A careful study was performed in evaluating other sources of error which contribute to the uncertainty in η_t .

The present high-precision result disagrees with a weighted average of previous experimental determinations [19] ($\eta_t = -0.054 \pm 0.0013$), but is in agreement with the recent measurement of George and Knutson [18] ($\eta_t = -0.0431 \pm 0.0025$). In addition, it is close to the average of experimental determinations made of η for ${}^3\text{He}$ ($\eta_{\text{He}} = -0.037 \pm 0.003$) [19].

The present η_t value is in agreement within errors with the theoretical value $\eta_t = -0.0432 \pm 0.0015$ obtained by the Sendai group [2] and is somewhat smaller than $\eta_t = -0.0460 \pm 0.001$ determined by the Los Alamos group [4]. Both groups extracted η_t by performing exact Faddeev-type calculations for several different two-body

and two-body plus three-body interactions. The results of recent experiments and calculations are summarized in Fig. 3. It is hoped that this result will contribute to better understanding of the three-body system.

ACKNOWLEDGMENTS

This work was supported by the U.S. Department of Energy through Grant No. DE-FG05-88ER40442. The authors wish to thank Dr. F. D. Santos and Dr. W. J. Thompson for helpful discussions in some aspects of the data analysis, and T. C. Black, J. C. Blackmon, E. R. Crosson, and K. A. Fletcher for their help in data acquisition. One of us (B.K.) would like to acknowledge partial financial support from the Fulbright Scholarship Program.

-
- [1] A. M. Eiro and F. D. Santos, *J. Phys. G* **6**, 1139 (1990).
 [2] S. Ishikawa and T. Sasakawa, *Phys. Rev. Lett.* **56**, 317 (1986).
 [3] S. Ishikawa and T. Sasakawa, *Few-body Systems* **1**, 143 (1988).
 [4] J. L. Friar, B. F. Gibson, D. R. Lehman, and G. L. Payne, *Phys. Rev. C* **37**, 2859 (1988).
 [5] R. K. Das, T. B. Clegg, H. J. Karwowski, and E. J. Ludwig, *Phys. Rev. Lett.* **68**, 1112 (1992).
 [6] T. E. O. Ericson and M. Rosa-Clot, *Nucl. Phys.* **A405**, 497 (1983).
 [7] L. D. Knutson, E. J. Stephenson, N. Rohring, and W. Haeberli, *Phys. Rev. Lett.* **31**, 1570 (1975).
 [8] L. D. Knutson, *Ann. Phys. (N.Y.)* **106**, 1 (1977).
 [9] R. P. Goddard, L. D. Knutson, and J. A. Tostevin, *Phys. Lett.* **118B**, 241 (1982).
 [10] N. L. Rodning and L. D. Knutson, *Phys. Rev. C* **41**, 898 (1990).
 [11] L. D. Knutson, P. C. Colby, and J. A. Bieszk, *Phys. Lett.* **85B**, 209 (1979).
 [12] L. D. Knutson, P. C. Colby, and B. P. Hichwa, *Phys. Rev. C* **24**, 411 (1981).
 [13] S. Sen and L. D. Knutson, *Phys. Rev. C* **26**, 257 (1982).
 [14] A. A. Ioannides, M. A. Nagarajan, and R. Shyam, *Phys. Lett.* **103B**, 187 (1981).
 [15] O. Karban and J. A. Tostevin, *Phys. Lett.* **103B**, 259 (1981).
 [16] E. Merz *et al.*, *Phys. Lett. B* **183**, 144 (1987).
 [17] C. M. Bhat, T. B. Clegg, H. J. Karwowski, and E. J. Ludwig, *Phys. Rev. C* **38**, 1537 (1988).
 [18] E. A. George and L. D. Knutson, *Phys. Rev. C* **48**, 688 (1993).
 [19] B. Vuaridel *et al.*, *Nucl. Phys.* **A449**, 429 (1989).
 [20] J. T. Londergan, J. C. E. Price, and E. J. Stephenson, *Phys. Rev. C* **35**, 902 (1987).
 [21] T. B. Clegg *et al.*, *Nucl. Instrum. Methods Phys. Res. Sect. A* (to be published).
 [22] S. A. Tonsfeldt, Ph.D. dissertation, University of North Carolina at Chapel Hill, 1980, available from University Microfilms International, 300 N. Zeeb Road, Ann Arbor, MI 48106, Order No. 8022515.
 [23] M. H. Macfarlane and S. C. Pieper, Argonne National Laboratory Report No. ANL-76-11, 1976 (unpublished).
 [24] W. W. Daehnick, J. D. Childs, and Z. Vrcelj, *Phys. Rev. C* **21**, 2253 (1980).
 [25] F. D. Becchetti and G. W. Greenlees, *Polarization Phenomena in Nuclear Reactions* (University of Wisconsin Press, Madison, 1971), p. 682.
 [26] G. R. Satchler, *Nucl. Phys.* **21**, 116 (1960).
 [27] P. W. Keaton and D. D. Armstrong, *Phys. Rev. C* **8**, 1692 (1973).
 [28] L. D. Knutson and W. Haeberli, *Phys. Rev. C* **12**, 1469 (1975).
 [29] J. E. Kammeraad and L. D. Knutson, *Nucl. Phys.* **A435**, 502 (1985).
 [30] J. A. Tostevin and R. C. Johnson, *Phys. Lett.* **124B**, 135 (1983); J. A. Tostevin, *Nucl. Phys.* **A466**, 349 (1987).
 [31] F. D. Santos, *Z. Phys. A* **295**, 73 (1980).
 [32] J. Rapaport, *Phys. Rep.* **87**, 25 (1982).
 [33] M. H. Lopes, J. A. Tostevin, and R. C. Johnson, *Phys. Rev. C* **28**, 1779 (1983).
 [34] T. Murayama, Y. Tagishi, T. Sakai, M. Tomizawa, H. Nishikawa, and S. Seki, *Nucl. Phys.* **A486**, 261 (1988).
 [35] R. P. Goddard and W. Haeberli, *Nucl. Phys.* **A316**, 116 (1979).
 [36] A. B. Smith, P. T. Guenther, and J. F. Whalen, *Nucl. Phys.* **A415**, 1 (1984).
 [37] E. Zijp and C. C. Jonker, *Nucl. Phys.* **A222**, 93 (1974).
 [38] S. Iijima and M. Kawai, *J. Nucl. Sci. Technol.* **20**, 77 (1983).
 [39] M. L. Roberts, P. D. Felsher, G. J. Weisel, Z. Chen, C. R. Howell, W. Tornow, and R. L. Walter, *Phys. Rev. C* **44**, 2006 (1991).
 [40] J. R. M. Annand and R. B. Galloway, *J. Phys. G* **11**, 1341 (1985).
 [41] J. A. Tostevin and R. C. Johnson, *Phys. Lett.* **85B**, 14 (1979).